SS-121
2251

ELECTRON-NEUTRINOS, ν_e

G. R. Kalbfleisch
Brookhaven National Laboratory

ABSTRACT

Electron (rather than muon) neutrino interactions are properly the ones to use in comparing results with e-p interactions.

Electron-neutrino fluxes from muons as well as kaons are crudely estimated. The muonic electron-neutrinos are more numerous than the kaonic ones but peak at a lower energy of course. Typical runs in the 25-foot (H or D) bubble chamber should yield several thousand ν_e interactions over the range 3-50 GeV in the current Nezrick beam. Identification of these events (electron track) should be easier than the corresponding muonic ones with a suitable plate array or track-sensitive target (Ne-H_2 or Ne-D_2) in the chamber. Some possibilities for greater ν_e yields in the future are indicated which will allow detailed studies of exotic processes (such as $\nu_e + e \rightarrow \nu_e + e$) also.

I. INTRODUCTION

Properties of the weak interaction are being explored with νN interactions. The copious high-energy ν source yields mainly muon neutrinos. Electron-neutrino interactions are also desired. The essential difference between electrons and muons has not yet been found. This difference may be found in the comparison of ν_eN and ν_μN interactions. In addition, ν_eN, rather than ν_μN data, is most properly compared with (extensive) eN data. Extensive μN data should exist later to properly compare with the more copious ν_μN data. Also, the expected (and assumed) decay modes of the muon

$$\mu^+ \rightarrow e^+ \nu_e \bar{\nu}_\mu ,$$

and

$$\mu^- \rightarrow e^- \bar{\nu}_e \nu_\mu$$

can be directly experimentally verified if a beam of muonically produced electron neutrinos is available.

A crude estimation of electron neutrinos in the current Nezrick beam is made in

this paper. The muonic source (considered here apparently for the first time) gives the dominant portion. The $K^{\pm} \rightarrow \pi^{o} e^{\pm} \nu_{e}$ reaction gives the higher energy electron-neutrinos as considered by BNL and CERN in their early experiments. The $K_{L}^{o} \rightarrow \pi^{\pm} \mu^{\mp} \nu_{\mu}$ and $\pi^{\pm} e^{\mp} \nu_{e}$ fluxes have not been done yet.

II. BRIEF SUMMARY

Only an outline of this (crude) estimation is given here. A detailed computer calculation should be undertaken since a reasonably useful flux is expected. The numerical results are worked out in Table I. The pion-muon sources are shown schematically in Fig. 1. Figure 2 gives the results as a ratio R versus momentum p_{ν}. This R is the factor to be applied to the calculated ν_{μ}^{π} spectrum to obtain the ν_{e} spectrum. In addition there is a contribution for K_{e3} decays. This factor has been applied to Nezrick's spectrum (see Fig. 4) and yields Fig. 3. The event yields for a run in the 25-foot bubble chamber are given later.

III. ν_{e} FROM MUON DECAY IN 600-METER π DRIFT SPACE

For every π decay, one obtains a μ as well as a ν_{μ}. For every such μ which decays, one obtains an e, ν_{e}, ν_{μ}, e.g.,

$$\pi^{+} \rightarrow \mu^{+} \nu_{\mu}$$
$$\quad \llcorner\!\rightarrow e^{+} \nu_{e} \bar{\nu}_{\mu} .$$

The decay rate of muons, however, is about 0.01 of that for pions of the same momentum. Thus a fraction of one percent might yield ν_{e} into the ν_{μ} beam. Let us calculate the ratio between ν_{e} and ν_{μ}; call this ratio R.

Consider the average angles for π and μ decay, the average decay paths for π and μ, and the relative solid angle subtended by the detector for ν's from pion and muon decay. These considerations yield the value of R. Averages of a quantity x will be denoted by $\bar{x}$.

The lab angle θ_{L} of a particle having a c.m. angle θ^{*} and velocity β^{*} from a decaying system traveling with velocity $\bar{\beta}$ is

$$\tan \theta_{L} = \frac{\sin \theta^{*}}{\left(\bar{\gamma} \cos \theta^{*} + \frac{\bar{\beta}}{\beta^{*}}\right)} .$$

A rough average angle in the lab system corresponds to $\theta^{*} = 90°$, i.e., $\theta_{L} \approx \beta^{*}/\bar{\eta}$. For a <u>massless</u> particle (γ or ν) we see that this is θ_{L} (m = 0) = $1/\bar{\eta}$. Thus the muon angle from π decay is $\overline{\theta_{\pi}^{\mu}} = \beta_{\mu}^{*}/\eta_{\pi} \approx m_{\pi}/p_{\pi} (p_{\mu}^{*}/m_{\mu})$. The average μ momentum is about $3/4\ p_{\pi} \approx (m_{\mu}/m_{\pi}) p_{\pi}$ (since p_{μ} ranges from ~1/2 p_{π} to p_{π}, as is well-known).

The average ν angles are $\overline{\theta^{\nu}_{\pi}} = 1/\eta_{\pi}$ and $\overline{\theta^{\nu}_{\mu}} = 1/\overline{\eta}_{\mu}$ (neglecting small effect of $\overline{\theta^{\mu}_{\pi}}$); i.e.,

$$\overline{\theta^{\nu}_{\mu}} = \frac{m_{\mu}}{\overline{p}_{\mu}} \simeq \frac{m_{\mu}}{\frac{m_{\mu}}{m_{\pi}} p_{\pi}} = \overline{\theta^{\nu}_{\pi}}.$$

That is, the solid angles subtended at the detector differ only in that the muon decays occur somewhat closer to the detector. The pion decay path is calculated from the pion momentum in the usual way, being the smaller of

$$\overline{\ell}_{\pi} = \eta_{\pi} c\tau_{\pi} = \frac{p_{\pi}}{m_{\pi}} c\tau_{\pi} \quad \text{or } 600 \text{ meters},$$

whereas the muon decay length is given essentially by the smaller of $\overline{\ell}_{\mu} = r/\theta^{\mu}_{\pi}$ or $600 - \overline{\ell}_{\pi}/2$ meters, where r is the pion decay drift tunnel radius* and 600 meters is the drift tunnel length. Finally, the $\overline{p}_{\nu}$ from π decay of momentum p_{π} is

$$\overline{p}_{\nu} \simeq 1/2\, \overline{p}_{\mu} \simeq 1/3\, p_{\pi}$$

for decays into

$$\theta_L = 0 \text{ to } \overline{\theta^{\nu}_{\mu,\pi}}$$

($\overline{p}_{\nu}$ over all angles $\simeq 1/4\, p_{\pi}$). These quantities are evaluated in Table I giving finally values of r (last column) as a function of $\overline{p}_{\nu}$. These are plotted in Fig. 2. A larger tunnel radius $r^{*} = D/2 = 1/2$ detector diameter would enhance low end by a factor of 3, but the ν_{μ} spectrum cuts off so fast below 3 GeV/c that this is effectively of no value. No change in tunnel radius is required for ν_{e}.

A similar calculation can be made for muons arising from $K_{\mu 2}$ decays. The

---

*A weighted average $\overline{\ell}^{W}_{\mu}$ over the decay path and forward peaked (lab) solid angle gives a result within 10%. This weighted average $\overline{\ell}^{W}_{\mu}$ is

$$\overline{\ell}^{W}_{\mu} = \frac{r}{\theta} + \frac{r}{2} \ell n \left[\frac{\theta + \sqrt{\theta^2 - \left(\frac{r}{L_1}\right)^2}}{\theta - \sqrt{\theta^2 - \left(\frac{r}{L_1}\right)^2}} \right], \quad \frac{r}{L_1} \leq \theta$$

$$= L_1, \quad \frac{r}{L_1} > \theta,$$

where $\theta = \overline{\theta^{\mu}_{\pi}}$ and L_1 = distance from mean π decay point to end of drift space (see Fig. 1).

value of r_K is about a factor of ten down from the values of r_π. This is due to the shorter muon decay path, since the mean muon angle from $K_{\mu 2}$ is about ten times larger than that for $\pi_{\mu 2}$. Thus r_K contributes negligibly relative to r_π at low momentum when the K/π ratio is also taken into account. At high momentum, r_K contributes negligibly compared to "copious" ν_e from K_{e3} decay (see Sec. V below).

IV. MUON DECAYS IN THE 300-METER Fe SHIELD

The high-energy muons have an appreciable path length in the Fe shield, allowing a contribution to the ν_e flux. For Fe, $dE/dx = a = 11.6$ MeV/cm = 1.16 GeV/m. The decay path $\bar{\ell}_\mu^{Fe}$ of a muon of momentum p_i ($p_i > 5$ GeV/c) slowed down to p_{cut} = 5 GeV/c ($\bar{p}_{\nu_e} \simeq 1/3\, p_\mu \sim 2$ GeV/c, corresponding to cutoff on ν_μ spectrum) is about

$$\bar{\ell}_\mu^{Fe} \simeq \frac{p_i - p_{cut}}{a}$$

The probability, P, for decay of such a muon is

$$P = \int_{p_i}^{p_{cut}} dP(p_\mu) = \int \frac{m_\mu}{p_\mu c\tau_\mu}\, dx$$

$$= \frac{m_\mu}{ac\tau_\mu}\, \ell n\left(\frac{p_i}{p_{cut}}\right)$$

since $p_\mu = p_i - ax$. For decays of 20-100 GeV/c μ's, the probability of decay is 2-5 times the 10^{-4} value allowed by the $\bar{\ell}_\mu^{Fe}$ if the muon were <u>not</u> slowed down. In particular, a 75 GeV/c muon (from 100 GeV/c π) would give 3×10^{-4} decay probability compared to 6×10^{-4} from drift space decay (see Table I). However, the average $\bar{p}_\mu$ is not 75 GeV/c, it is

$$\bar{p}_\mu = \frac{1}{P}\int_{p_i}^{p_{cut}} \frac{m_\mu\, dx}{c\tau_\mu} = \frac{p_i - p_{cut}}{\ell n\left(\frac{p_i}{p_{cut}}\right)}$$

which is ~ 27 GeV/c yielding a $\bar{p}_\nu \sim 9$ GeV/c. The relative rate of such low-energy ν_e's is much higher (Table I) 60×10^{-4} even excluding the increase of ν_μ spectrum at lower p. Thus decays in the Fe shielding can be neglected.

V. ν_e FROM $K_{e3}^{\pm}$ DECAY

The problem here is simpler. The branching fractions

$$K^\pm \to \mu^\pm \nu_\mu \qquad 64\%$$

$$K^\pm \to \pi^o e^\pm \nu_e \qquad 5\%$$

give ν_e/ν_μ in ratio 5/64 ≃ 0.08 into the same solid angle (different mode of same momentum $K^\pm$ and $\theta_K^\nu = 1/\eta_K$). However, the average $\overline{p}_\nu$ is different for the two modes, since one is a two-body and the other a three-body decay. The p_ν^* (or p_ν^{*max}) for both modes is ≃ 0.23 GeV/c. For the three-body mode, the p_ν^* spectrum is approximately linear from 0 to p^{*max}, i.e.,

$$\overline{p^*_{K_{e3}}} \simeq 2/3\, p^{*max} \simeq 0.15 \text{ GeV/c}.$$

For

$$K_{\mu 2}\ p_\nu^{lab} \simeq 0 \text{ to } 0.9\, p_K$$

$$K_{e3}\ p_\nu^{lab}\ (\overline{fnp^*}) \simeq 0 \text{ to } 0.46\, p_K,$$

so that

$$\overline{p_K^{\nu_e}} \simeq 0.5\, \overline{p_K^{\nu_\mu}}$$

Thus $N(\nu_e^K)$ at p_ν is 0.08 of $N(\nu_\mu^K)$ at $2p_\nu$, i.e.,

$$N_{\nu_e}^{K^\pm}(p_{\nu_e}) = 0.08\, N_{\nu_\mu}^{K^\pm}(2p_{\nu_e}).$$

VI. ν_e FROM $K_L^o \to \pi^o e^\pm \nu_e$ DECAY

The branching ratios are:

$$K_L^o \to \pi^o e^\pm \nu_e \qquad 28\%$$

and

$$K_L^o \to \pi^o \mu^\pm \nu_\mu \qquad 38\% \qquad \text{respectively.}$$

The solid angle and momentum spectra are almost the same for both ν_e and ν_μ here since p^{*max} for each mode is approximately the same (0.22 GeV/c). Thus the ν_e spectrum for K_L^o decays is 0.7 that of ν_μ. The unfocused $K_L^o \to \nu_\mu$ spectrum has not been calculated by Nezrick. We will for now ignore the ν_e contribution corresponding to that source, although it may be ≃ 10% of all ν_e.

VII. ν_e FLUX

The ν_e flux from μ^+ and K^+ are given in Fig. 3 using the results of Secs. III and V and the Nezrick ν_μ spectrum of Fig. 4.

The total ν_e spectrum goes from about 3 to 50 GeV/c with 80% resulting from the muonic decay.

VIII. ν_e EVENT RATES

Roe's assumptions for a 10^6 picture run of the 25-foot bubble chamber with 21-foot deuterium length was used for this estimation. Using

$$\sigma_{tot} = 0.8\, E^{\nu}_{GeV} \times 10^{-38}\ cm^2$$

as an estimate, Roe obtains about 10^6 total ν_μ N interactions, and we shall also obtain about 6,000 ν_e N interactions of all kinds (similar to ν_μ reactions, replacing μ out with e). About 2,200 will be from 3-10 GeV/c, 2,200 from 10-20 GeV/c and 1,600 from 20-50 GeV/c. Also 65% derive from muonic ν_e and the 35% balance from kaonic ν_e.

Also, since the $\bar{\nu}_\mu$ spectrum is about one-third of ν_μ spectrum, one will obtain similarly about 2,000 ν_e N interactions when tuned for π^- antineutrinos.

Thus substantial ν_e N physics can be done even in the current neutrino proposals. For the future, Palmer quotes ×10 fluxes on low-energy neutrinos at BNL-AGS and ×100 for low-energy NAL 25-foot runs. "Muon focusing" in the drift space may allow for designing yet another ×10 factor. I shall think about this in the coming months. At this level, the comparison of ν_e and ν_μ should be very good. The "focused muon" beam might be arranged so as to have a negligible pionic ν_μ background. Then since the muonic $\bar{\nu}_\mu$ and ν_e (for μ^+, and conversely for μ^-) spectra are the same, the direct experimental test of the assumption $\mu^+ \to e^+ \nu_e \bar{\nu}_\mu$ indicated earlier can be made. In addition, exotic reactions, like "diagonal" $\nu_e e \to \nu_e e$ will give substantial rates for many interesting results.

IX. ANALYSIS OF ν_e EVENTS

Although only ~ 0.6% of the ν interactions are ν_e, the analysis should be relatively as easy as the muon analysis if one uses a double chamber (D_2 and Ne-D_2) or a suitable plate array to identify the electrons by their showers.

Table I. Pion → Muon → Electron-Neutrino Decay (See Fig. 1).

p_π(GeV/c)	$\bar{\theta}^\mu_\pi$ (rad)	$\bar{\ell}_\pi$ (m)	$\bar{\ell}_\mu$ (m)	$\bar{p}_\nu$(GeV/c)	B[a]	μ (Decay Fraction)	$R(\nu_e^\mu/\nu_\mu^\pi)$
1	0.042	56	20[b]	0.33	1[b]	4.5×10^{-3}	4.5×10^{-3}[b]
2	0.021	112	40[b]	0.67	1[b]	4.5×10^{-3}	4.5×10^{-3}[b]
5	0.0084	280	100[b]	1.67	1.2[b]	4.5×10^{-3}	5.4×10^{-3}[b]
10	0.0042	560	200[b]	3.3	1.4[b]	4.5×10^{-3}	6.1×10^{-3}[b]
20	0.0021	600	300	6.7	1.8	3×10^{-3}	5.4×10^{-3}
50	0.00084	600	300	16.7	1.0	1.2×10^{-3}	1.2×10^{-3}
100	0.00042	600	300	33	1.0	0.6×10^{-3}	0.6×10^{-3}
200	0.00021	600	300	67	1.0	0.2×10^{-3}	0.3×10^{-3}

[a] $B = [(\text{larger of } D/2 \text{ or } \theta_\pi y_\pi)/(\text{larger of } D/2 \text{ or } \theta_\mu y_\mu)]^2 = (\Delta\Omega_{\nu_e})/(\Delta\Omega_{\nu_\mu})$ where D/2 = 2.5 m and y_π and y_μ distances of mean π and μ decay points from end of shield (see Fig. 1).

[b] For larger tunnel (radius ≥ D/2 or tapered to this size at shield) the fluxes for p_π = 1, 2, 5, 10 GeV/c are increased by factors of 3, 3, 3, 1.5 respectively.

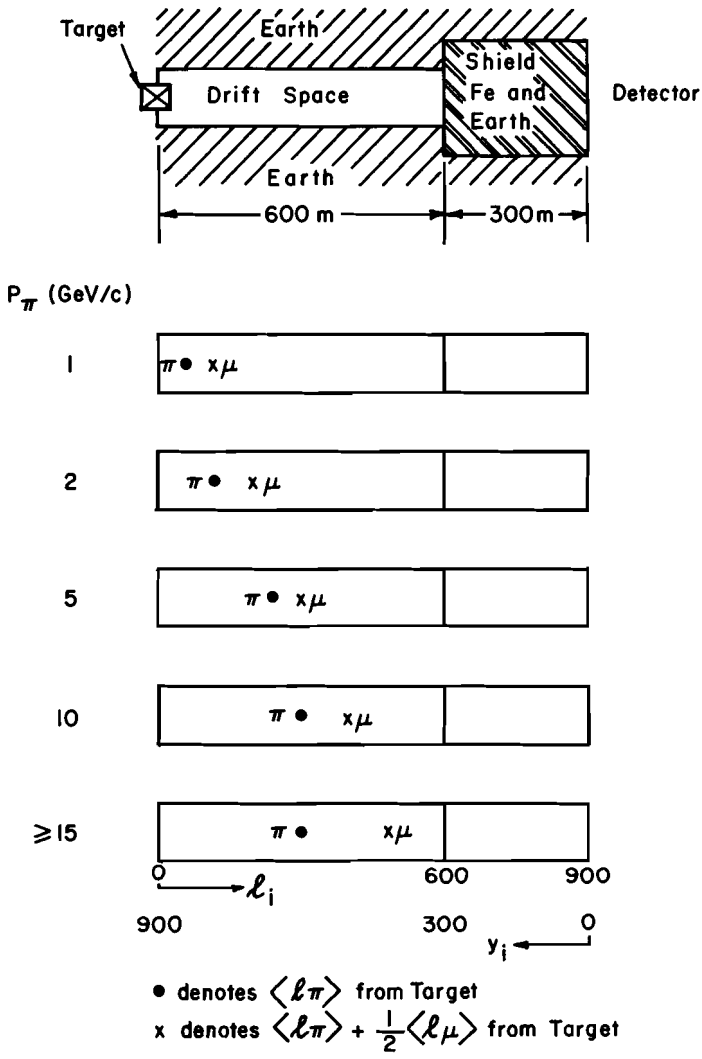

Fig. 1. Average decay positions of pions and muons in the neutrino tunnel (see Table I). Distances are measured from the target end.

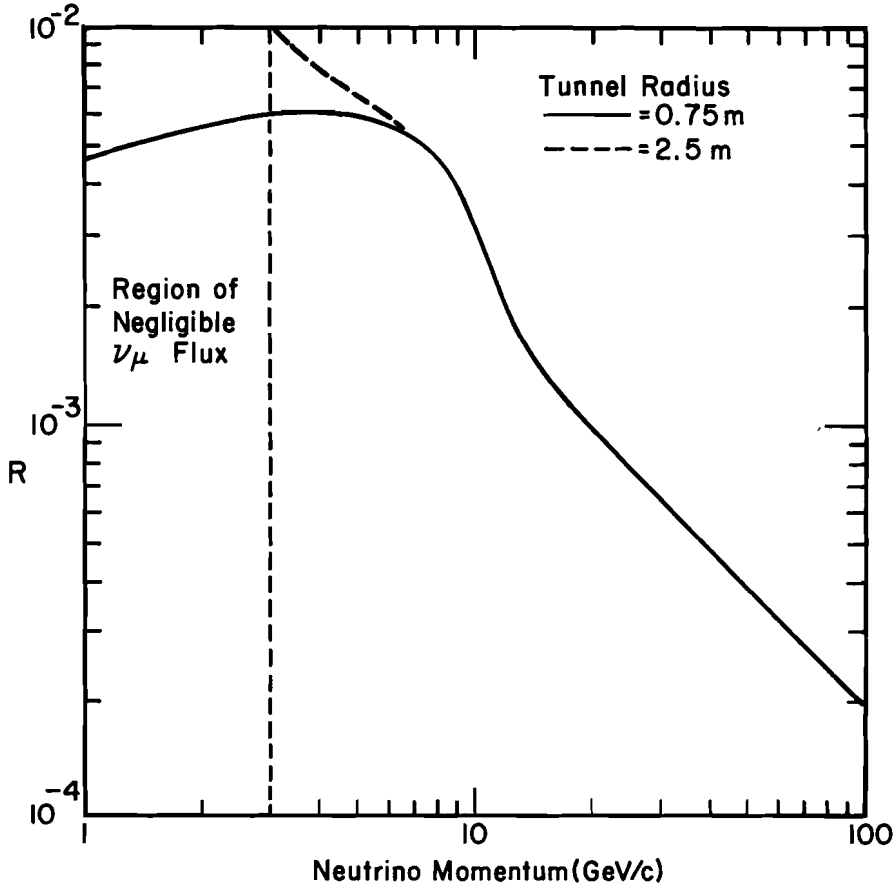

Fig. 2. Spectrum of the ratio of electron to muon neutrinos, $R = N[\nu_e(p)]/N[\nu_\mu^\pi(p)]$.

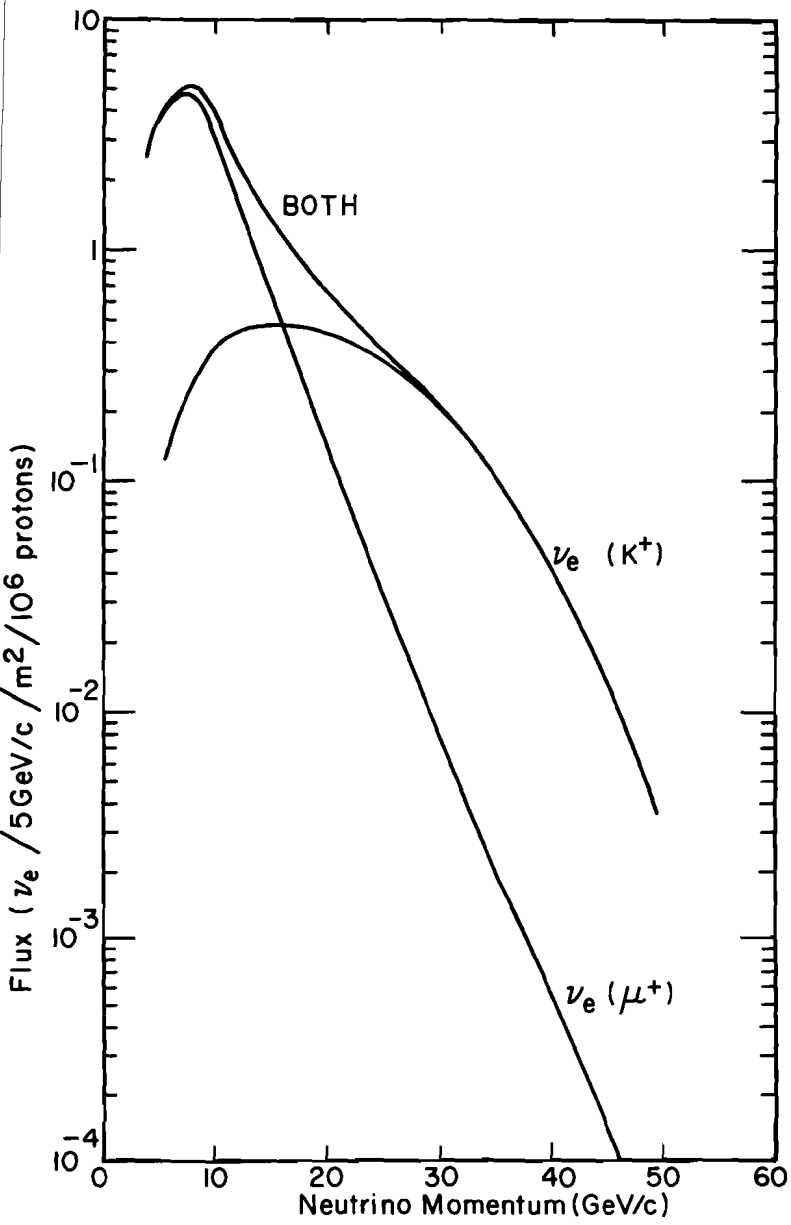

Fig. 3. Spectra of electron neutrinos.

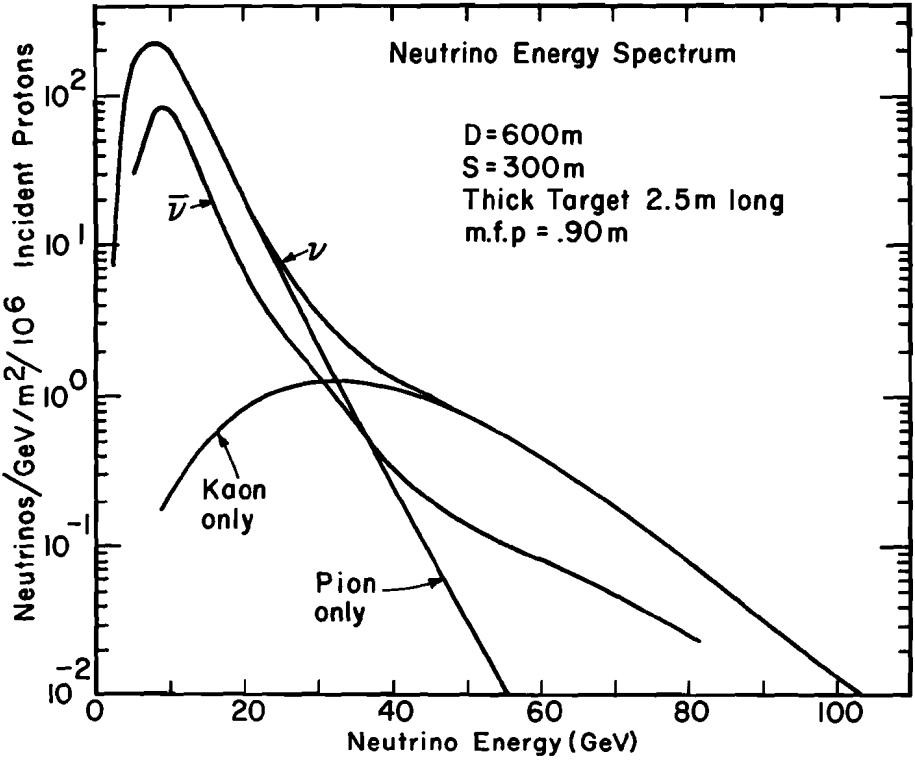

Fig. 4. Neutrino spectra used to calculate spectra of Fig. 3.